

## Estimation of lunar FeO abundance based on imaging by LRO Diviner

Xiao Tang<sup>1,2</sup>, Xiao-Xing Luo<sup>3</sup>, Yun Jiang<sup>2</sup>, Ao-Ao Xu<sup>4</sup>, Zhen-Chao Wang<sup>5</sup>, Xue-Wei Zhang<sup>1</sup>, Yuan Chen<sup>1</sup>, Xiao-Meng Zhang<sup>1</sup>, Wei Cai<sup>1</sup> and Yun-Zhao Wu<sup>1,6</sup>

<sup>1</sup> School of Geographic and Oceanographic Sciences, Nanjing University, Nanjing 210023, China; [wu@nju.edu.cn](mailto:wu@nju.edu.cn)

<sup>2</sup> Key Laboratory of Planetary Sciences, Chinese Academy of Sciences, Nanjing 210008, China

<sup>3</sup> East China Mineral Exploration and Development Bureau, Nanjing 210007, China

<sup>4</sup> Macao University of Science and Technology, Macao, China

<sup>5</sup> School of Earth Sciences and Engineering, Nanjing University, Nanjing 210023, China

<sup>6</sup> Jiangsu Center for Collaborative Innovation in Geographical Information Resource Development and Application, Nanjing 210023, China

Received 2015 March 8; accepted 2015 August 21

**Abstract** Understanding the abundance and distribution characteristics of FeO on the surface of the Moon is important for investigating its evolution. The current high resolution maps of the global FeO abundance are mostly produced with visible and near infrared reflectance spectra. The Christiansen Feature (CF) in mid-infrared has strong sensitivity to lunar minerals and correlates to major elements composing minerals. This paper investigates the possibility of mapping global FeO abundance using the CF values from the Diviner Lunar Radiometer Experiment aboard the Lunar Reconnaissance Orbiter (LRO) mission. A high correlation between the CF values and FeO abundances from the Apollo samples was found. Based on this high correlation, a new global map ( $\pm 60^\circ$ ) of FeO was produced using the CF map. The results show that the global FeO average is 8.2 wt.%, the highland average is 4.7 wt.%, the global modal abundance is 5.4 wt.% and the lunar mare mode is 15.7 wt.%. These results are close to those derived from data provided by Clementine, the Lunar Prospector Gamma Ray Spectrometer (LP-GRS) and the Chang'e-1 Interference Imaging Spectrometer (IIM), demonstrating the feasibility of estimating FeO abundance based on the Diviner CF data. The near global FeO abundance map shows an enrichment of lunar major elements.

**Key words:** astrochemistry — planets and satellites: detection — methods: data analysis — infrared: general

### 1 INTRODUCTION

Understanding the chemical composition of the Moon will provide insight into lunar formation. Iron is one of the major elements that strongly influences composition and structure of silicate minerals on the lunar surface (Wilcox et al. 2005). Knowing the iron abundances and distribution is meaningful for study of the origin and evolution of the Moon (Lucey et al. 1995; Taylor 1987). Iron mainly exists in ilmenite, olivine and pyroxene, all of which are widely distributed in lunar mare basalts (Anderson & Kovach 1972; Anderson 1973). For the past few years, data from Clementine and the Chang'e-1 Interference Imaging Spectrometer (IIM) have been used to derive increasingly refined estimates of FeO abundances (Lucey et al. 1995, 1998, 2000; Lawrence et al. 2002; Gillis et al. 2004; Wu et al. 2012; Wu 2012). These studies used visible and near infrared spectra. Data from the Lunar Prospector Gamma Ray Spectrometer (LP-GRS) have also been used to estimate FeO content, but the resolution is low which makes it difficult to investigate local areas (Lawrence et al. 2002;

Gillis et al. 2004). There has been no global FeO map with high resolution derived from the mid-infrared bands until now.

Mid-infrared remote sensing, with wavelengths between 3  $\mu\text{m}$  and 25  $\mu\text{m}$ , has a long history in the field of lunar and planetary science and plays an important role in classification and determination of lunar minerals and elemental content (Ohtake et al. 2009; Kusuma et al. 2012). Mid-infrared remote sensing is a good technique for chemical composition research which has been studied in visible and near-infrared. Early lunar remote sensing observations in mid-infrared lacked enough spatial resolution and coverage for global scale research. The spectral resolution was not high enough for identifying the unique spectral characteristics of minerals.

Mid-infrared remote sensing spectra of lunar minerals include a prominent emission maximum near 8  $\mu\text{m}$ , known as the “Christiansen Feature” (CF). Conel (1969) first pointed out that the CF of mid-infrared spectra could be used as an index for the identification of silicate mineral composition. The inflection point wavelength (CF value) is

sensitive to the degree of polymerization of silicate minerals (Logan et al. 1973), which is strongly influenced by Fe, the major cation in the minerals. The FeO abundances of several lunar pyroclastic deposits (LPDs) have been estimated based on CF data (Allen et al. 2012). The purpose of this study is to investigate whether high correlation exists at a global scale and to produce a global FeO map of the Moon using mid-infrared remote sensing technology. This research will advance knowledge about FeO available from the mid-infrared bands.

## 2 DATA AND METHOD

### 2.1 Christiansen Feature

CF occurs at the wavelength just shorter than the position of the fundamental frequency of vibration where the absorption is relatively weak. In this area, the index of refraction of a mineral grain changes quickly and is comparable to the surrounding medium, resulting in a backscatter minimum. Both absorption and the backscatter minimum hence result in an emission maximum (Salisbury & Walter 1989; Betts 1997).

The sensitivity of CF to lunar silicate mineralogy was demonstrated shortly after the Apollo samples were collected, which makes it an appropriate index for distinguishing major minerals on the lunar surface, such as feldspar, pyroxene and olivine (Paige et al. 2010; Korotev et al. 1996). The CF wavelength of a silicate mineral depends on the silicate framework and chemical composition (Betts 1997). As for a silicate framework, the CF wavelength is affected by the silicate polymerization of a silicate mineral. Higher polymerization results in higher frequencies of vibration, which makes the position of the fundamental vibration bands of silicates shift to shorter wavelength and thus the CF wavelength value will decrease (Paige et al. 2010). Laboratory measurements of minerals in a simulated lunar environment show how different CF wavelengths change with different degrees of polymerization (Fig. 1) (Ohtake et al. 2009). For example, the CF wavelength for plagioclase is 7.84  $\mu\text{m}$ , for pyroxene it is 8.25  $\mu\text{m}$  and for olivine it is 8.67  $\mu\text{m}$ . As for the chemical composition, different minerals have different elemental contents. Pyroxene and olivine have higher iron content while feldspar has lower iron content. The CF position shifts to a longer wavelength with an increase in mafic content of the silicate (Allen et al. 2012).

### 2.2 Data

Diviner, which is onboard NASA's Lunar Reconnaissance Orbiter (LRO), is a multi-channel radiometer that maps the reflected solar radiation and emitted thermal radiation from the lunar surface at a resolution of 200 m/pixel at the lunar equator (Ohtake et al. 2009). The detector's geometric Instantaneous Field of View (IFOV) is 320 m on the ground in track and 160 m on the ground cross track at an altitude of 50 km. The swath width is  $\sim 3.4$  km (Paige

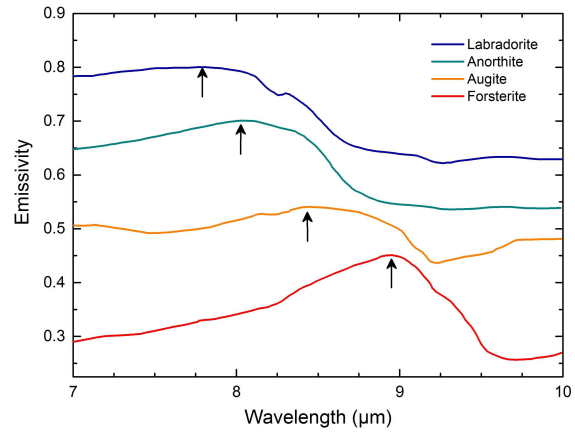


**Fig. 1** The mid-infrared spectra (7–10  $\mu\text{m}$ ) of several minerals (Ohtake et al. 2009). Arrows mark the position of the CF wavelength, showing the systemic shift of CF wavelength with silicate polymerization.

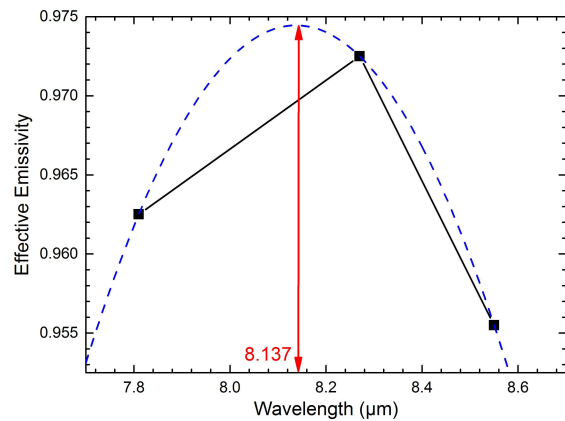


**Fig. 2** A three point spectrum of an Apollo 16 sample that was previously recorded by Diviner (Greenhagen et al. 2010). The CF wavelength is calculated by using a parabolic fit to the three points.

et al. 2010). The multispectral push broom sensor that is part of Diviner collects information in nine spectral channels. Channels 3–5 have relatively narrow pass-bands near 8  $\mu\text{m}$  and sufficient signal-to-noise ratio to allow accurate spectral location of the emissivity maximum, which are designed to measure the CF and characterize compositional information about silicate.

The Diviner science team calculated the CF wavelength from the original channels 3–5 to obtain the level 3 CF data. They first binned and averaged each radiance and converted them to an emissivity value. Then a three-point emissivity spectrum was solved quadratically to determine the maximum emissivity, where the corresponding position refers to the CF wavelength (Fig. 2) (Ohtake et al. 2009; Paige et al. 2010; Greenhagen et al. 2010). The current CF mosaic data cover the lunar surface between 60°N and 60°S (Greenhagen et al. 2010), and the range of wavelength is approximately between 8.00  $\mu\text{m}$  and 8.40  $\mu\text{m}$  at

a high resolution of 0.02  $\mu\text{m}$  (Kusuma et al. 2012). The reader is referred to Paige et al. (2010) for a detailed explanation of the Diviner and CF data.

### 2.3 Estimating FeO Abundance

The mid-infrared spectra of Apollo samples measured in RELAB show that the CF wavelength of laboratory measurements of samples is strongly correlated with FeO abundance, and the CF wavelength of orbital mid-infrared measurement is linearly correlated to published FeO abundance of Apollo samples (Korotev et al. 1996). This paper aims to extend this correlation from Apollo samples to the lunar surface. That is, a correlation between CF wavelengths derived from the orbital measurement and FeO abundance of the lunar surface will be built and, further, the FeO abundance of the Moon is estimated with this correlation.

Generally, two types of models can be used to estimate FeO abundance. One is based on the statistics of relationships between spectral reflectance and compositional data, and the other is to parameterize spectral properties sensitive to iron (Wu 2012). In this paper, the second method is applied for estimating the FeO abundance of the Moon. The FeO contents of returned soils from the Moon (Lucey et al. 2000; Blewett et al. 1997) and feldspathic lunar meteorites (Korotev et al. 2003) are used as ground truth. The CF value of the landing site and lunar farside highlands (between 90°E and 270°E) were extracted from the Diviner mosaic. Starting with the latitude and longitude of each imaged location, together with published traverse maps, the CF values were manually extracted from 25 imaged locations using the Diviner CF mosaic. Using this method of matching to identify imaged locations is more accurate than relying on a latitude and longitude based approach with spacecraft pointing information. In order to avoid all the sampled locations being from the nearside of the Moon and no plagioclase being sampled, a sample from the lunar farside highlands (LFH) was included. The CF values of almost the whole LFH were averaged as the CF value of the LFH. The FeO abundance of the LFH adopts the average of lunar highland meteorite samples (Wu 2012; Glotch et al. 2010). A detailed list of these samples is given in Table 1. Finally, a good correlation between FeO abundance and CF value for the 26 points was established. The linear fitting proved to be the best approach in estimating FeO abundances (Fig. 3).

## 3 RESULTS AND DISCUSSION

The result of the linear fitting with Diviner CF wavelengths and FeO abundances is shown in Figure 3. The regression equation is  $\text{FeO} = 65.47 \times \text{CF} - 527.938$ . The correlation index is 0.89, showing there is a high correlation between CF wavelength and FeO abundances. The standard errors of parameter a (-527.938) and b (65.47) in the model are 37.0 and 4.5 respectively. The resolution of CF data is 0.02  $\mu\text{m}$ , so the error of the derived FeO is 1.3 wt.%.

**Table 1** The Sampling Selected for Estimating FeO Abundances (Paige et al. 2010; Wu 2012; Blewett et al. 1997).

Sample	Pixels	CF wavelength ( $\mu\text{m}$ )	FeO abundance (wt.%)
Apollo 11	1 × 1	8.285	15.8
Apollo 12	1 × 1	8.313	15.4
Apollo 14-LM	3 × 3	8.255	10.5
Apollo 14-Cone	1 × 1	8.220	10.3
Apollo 15-LM	3 × 3	8.252	15.0
Apollo 15-S2	1 × 1	8.238	11.5
Apollo 15-S6	1 × 1	8.265	12.1
Apollo 15-S7	1 × 1	8.253	13.9
Apollo 15-S8	1 × 1	8.263	15.2
Apollo 15-S9	1 × 1	8.305	16.9
Apollo 16-LM	1 × 1	8.162	5.6
Apollo 16-S1	1 × 1	8.158	5.4
Apollo 16-S4	1 × 1	8.100	4.6
Apollo 16-S5	1 × 1	8.171	5.9
Apollo 16-S6	1 × 1	8.173	6.0
Apollo 17-S2 & LRV4/S2	6 × 6	8.213	8.6
Apollo 17-S3	1 × 1	8.206	8.7
Apollo 17-S6	1 × 1	8.252	10.7
Apollo 17-S7	1 × 1	8.247	11.6
Apollo 17-S9	1 × 1	8.329	15.4
Apollo 17-LRV1-3	8 × 8	8.284	14.8
Apollo 17-LRV5-6	2 × 2	8.232	10.1
Apollo 17-LRV7-8	4 × 4	8.302	15.9
Apollo 17-LRV9	1 × 1	8.263	14.6
Apollo 17-LRV12	1 × 1	8.320	17.4
LFH*	1 × 1	8.123	4.4

Notes: LFH FeO abundance is averaged by feldspathic lunar meteorites: ALHA 81005, MAC 88105, QUE 93069, Yamato 86032, DaG 262, DaG 400, Dhofar 025 and NWA 482 (Korotev et al. 1996).

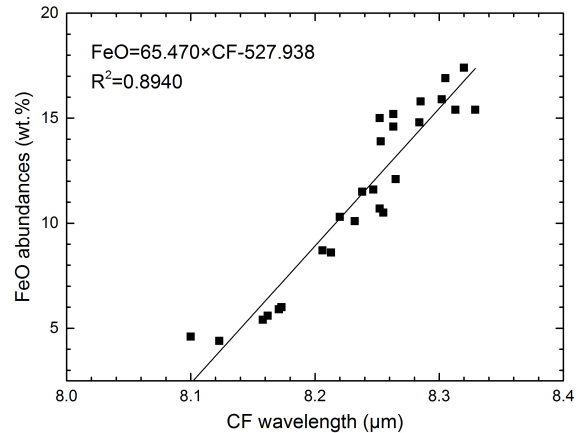


**Fig. 3** The scatter plot of FeO abundances and CF wavelength for 26 points.

for the propagation of error. According to the regression line equation, the FeO abundance map of the Moon was produced using Diviner CF data between 60°N and 60°S (Fig. 4). Red represents higher iron content and blue represents lower iron content. The highlands and mare are each clearly visible in Figure 4.

Figure 5 shows that the statistical histogram of global FeO has a bimodal distribution. The first peak represents the highland area and the other represents the mare area. The convexity of the second peak is weaker than the first

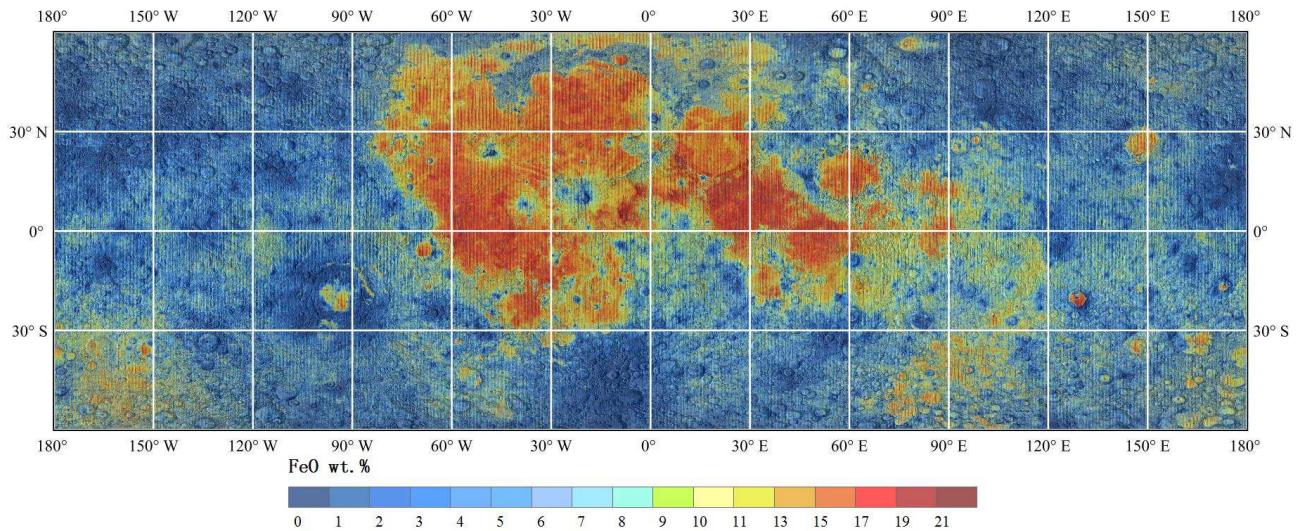


**Fig. 4** The FeO map derived from Diviner CF data.

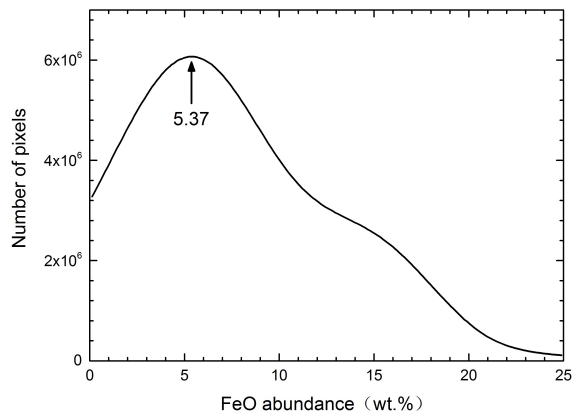


**Fig. 5** The global histogram of FeO abundance.

peak, corresponding to less coverage of mare basalts compared with highlands. Generally, the histogram of FeO derived from Diviner CF data is similar to those from Clementine and IIM data (Lucey et al. 1998; Wu et al. 2012; Wu 2012).

Table 2 shows the comparison between our results and those from Clementine, LP-GRS and IIM. The average FeO abundance of the whole nearside of the Moon ( $\pm 60^\circ$ ) derived in this paper is 8.2 wt.%, which is lower than the average abundance of 8.6 wt.% (Lucey et al. 2000), and a little higher than average abundance values of 8.1 wt.% and 7.7 wt.% (Lawrence et al. 2002). The modal abundance of 5.4 wt.% is close to that of Lucey et al. (2000) (5.7 wt.%) and 5.57 wt.% given by Wu (2012), but higher than the modal abundance of 4.7 wt.% published by Lawrence et al. (2002) and 3.65 wt.% provided by Wu et al. (2012). The average FeO abundance of highlands is the same as that of Wu et al. (2012), and similar to Lucey et al. 2000 and Lawrence et al. 2002. The FeO abundance of feldspathic

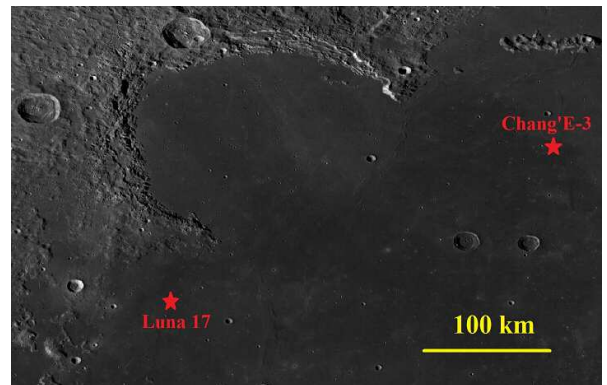


**Fig. 6** The LROC Wide Angle Camera (WAC) image of north-west Imbrium with the landing sites of Chang'e-3 and Luna 17 shown.

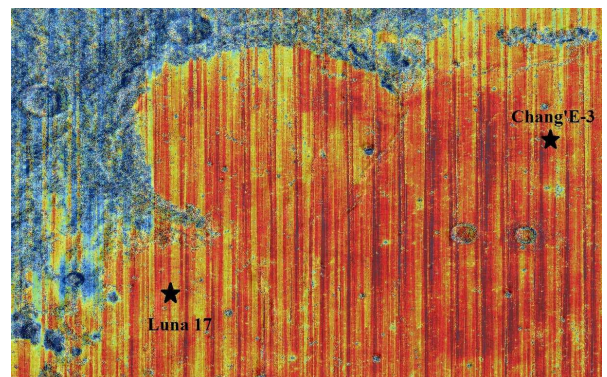


**Fig. 7** FeO abundance derived from the Diviner CF map in the same area as shown in Fig. 6.

lunar meteorites lies in a range of 4.3–6.1 wt.% (Korotev et al. 2003). The average FeO abundance of highlands in this paper is 4.7 wt.%. Overall, the comparison shown

**Table 2** The Comparison of FeO Derived From Diviner with Those of Clementine, LP-GRS and IIM Data

Author	Data	Global avg.	Highland avg.	Global mode	Mare mode
Lucey et al. 2000	Clementine	8.6	4.5	5.8	–
Lawrence et al. 2002	Clementine	8.1	5.1	5.7	–
Gillis et al. 2004	Clementine	8.6	4.4	5.7	–
Lawrence et al. 2002	LP-GRS	7.7	4.3	4.7	–
Wu et al. 2012	IIM	–	4.73	3.65	15.09
Wu 2012	IIM	–	–	5.57	15.27
This paper	Diviner	8.2	4.7	5.4	15.7

**Table 3** Maximum FeO Abundance of Major Lunar Mare

Mare	Maximum FeO abundance (wt.%)	Latitude (°)	Longitude (°)
Mare Serenitatis	23.809	22.8906	11.2188
Mare Orientale	21.382	–22.4922	–93.1719
Oceanus Procellarum	24.194	10.7109	–58.1563
Mare Tranquillitatis	24.176	8.5000	34.5703
Mare Moscoviense	22.110	22.8125	146.8281
Mare Humorum	23.406	–19.9297	–38.0938
Mare Crisium	23.961	18.3906	65.9766
Mare Imbrium	24.325	39.4297	–27.7266
Mare Nubium	21.175	–25.6875	–16.0938

above suggests that the FeO derived from Diviner CF data agrees with the results from optical and gamma ray data.

The maximum iron abundances of major lunar maria are shown in Table 3. They indicate that northwest Imbrium, south Procellarum and Mare Tranquillitatis have higher FeO with values of 24.3 wt.%, 24.2 wt.% and 24.2 wt.% respectively. Mare Orientale and Mare Nubium have relatively lower FeO abundances with values of 21.4 wt.% and 21.2 wt.%, respectively. The FeO abundances of major lunar maria are not very different. The average FeO abundance of Tsiolkovskiy, a major mare on the lunar farside, is 15.3 wt.%, which is close to the corresponding values of maria on the lunar nearside.

Mare Imbrium is located in the Procellarum KREEP Terrane (PKT). The average FeO of Imbrium is 15.98 wt.%. The FeO abundance at the Chang'e-3 landing site is 17.17 wt.%. The FeO abundance at the Luna 17 landing site is 18.21 wt.%, which is higher than at the Chang'e-3 landing site. These values are lower than those from Clementine, IIM and LP-GRS. The global map of olivine-rich non-mare basalts on the Moon shows that the north wall of Sinus Iridum contains about 70%–80% olivine. The Moon Mineralogy Mapper (M3) Integrated Band Depth (IBD) color composite map also displays olivine-rich rocks on the north wall. However, the FeO abundance map does not clearly feature the iron-rich area on the north wall of Sinus Iridum. A possible interpretation is that the CF value of a mixed mineral is nonlinear. A mixture of olivine and plagioclase would have an intermediate value similar to pyroxene due to this nonlinear behavior. It will not move the CF to a longer wavelength by a corresponding amount when the olivine contents of the mixture increase.

The FeO range of the selected samplings cannot cover all of the lunar surface, so we can extrapolate our derived

FeO abundance. We try to collect as many samples as possible for constructing the model. As shown in Table 1, we included a sample from the LFH from meteorites which represent the lowest FeO on the Moon (4.4 wt.%). The samples from the Apollo 17 landing site which mostly represent the highest FeO on the Moon (17.4 wt.%) were also included. By a global comparison with previous results, we believe the range used in this study (4.4–17.4 wt.%) can represent most of the lunar FeO abundances.

In some small areas, the FeO abundances are out of the range of 4.4–17.4 wt.%, but they do not deviate much. The lowest value of derived FeO (with expected error) is about 2.1 wt.% which can be extrapolated to 2.3 wt.%, and its highest value is about 23.9 wt.% which can be extrapolated to 6.5 wt.%. Unfortunately, the error associated with the extrapolation cannot be estimated in this study because we do not know the true value of lunar FeO abundance.

Lunar pyroclastic deposits are dark material-enriched glass beads and iron. Sample analysis and studies using simulation have indicated that LPDs probably represent the deepest-sourced and most primitive magmas on the Moon (Howard 1973). The FeO of Aristarchus, Sulpicius Gallus and Rima Fresnel estimated by Allen et al. (2012) are 19.3 wt.%, 21.6 wt.% and 16.7 wt.% respectively. This study demonstrates that the FeO abundances of these deposits are 18.1 wt.%, 20.0 wt.% and 15.8 wt.% respectively. Abundances of three LPDs all have about a 1 wt.% deviation. This is possibly because when we established the model we added the sampled point from the LFH. This point represents the area associated with the highlands and moves the regression line towards low Fe.

The temperature of the lunar surface has some important effects on CF wavelength. The spectra measured in a simulated lunar environment show that increasing temper-

ature shifts the CF wavelength to lower values, thus increasing spectral contrast. All data in this paper were taken near mid-day to maintain consistent lighting and soil temperatures, so the temperature does not affect the derived FeO abundances too much. We did not use a model to normalize the effects of latitude, which might affect the accuracy of our derived results.

The CF data calculated by just three 8- $\mu\text{m}$  channels lack sufficient spectral resolution for producing a more precise CF wavelength. Obviously, errors from data in an arbitrary channel would affect the estimation of results from the CF wavelength. It may be difficult to use these data over a small scale, but the high signal to noise ratio of Diviner makes these data precise enough to study at large scale.

The maturity of the soils also has an important effect on CF wavelength. The CF values shift to longer wavelengths with increasing maturity, which makes it difficult to obtain a precise CF value. The maturity is defined as optical properties of the surface that are changed in systematic ways due to the long-term effects of space weathering, such as spectral darkening, reddening and subdued absorption bands (Hapke 2001). In this paper, the CF values of the relatively mature surface were selected according to the maturity of samples. In this paper, the selected samples and CF values are all from lunar soil and are relatively mature. So, the derived FeO abundances of fresh craters are less precise than those of lunar surface soil.

#### 4 CONCLUSIONS

The CF in mid-infrared is sensitive to lunar minerals. This paper obtained a high correlation between the CF values and the FeO abundances on a nearly global scale. The linear fitting is good enough to estimate FeO abundances between 60°N and 60°S. The global FeO abundance was calculated using mid-infrared bands based on the high correlation. A new map of FeO abundances was produced.

The global FeO average derived from Diviner CF data is 8.2 wt.% and the highland average is 4.7 wt.%. The global modal abundance is 5.4 wt.% and that for the corresponding lunar mare mode is 15.7 wt.%. The statistical indexes of our estimated results derived from Diviner CF data are similar to those from Clementine, LP-GRS and IIM, which demonstrate the reliability and accuracy of our results. According to the global results, we obtained the maximum FeO of several major lunar mares, the FeO abundances of the Chang'e-3 landing site and the Luna 17 landing site. These results will provide useful information for lunar geologic research. A good estimation of the abundances and distributions of major elements will provide deep insight into the evolution history and composition of the Moon, and also lays a solid foundation for exploring lunar resources in the future.

**Acknowledgements** Acknowledgement is given to the Geosciences Node of NASA's Planetary Data System and Diviner science team for providing Diviner and CF

data. This research was supported by the National Natural Science Foundation of China (41172296 and 41422110), the Science and Technology Development Fund of Macau (048/2012/A2), and the Key Research Program of the Chinese Academy of Sciences (KGZD-EW-603).

#### References

- Allen, C. C., Greenhagen, B. T., Donaldson Hanna, K. L., & Paige, D. A. 2012, *Journal of Geophysical Research (Planets)*, 117, E00H28
- Anderson, D. L. 1973, *Earth and Planetary Science Letters*, 18, 301
- Anderson, D. L., & Kovach, R. L. 1972, *Physics of the Earth and Planetary Interiors*, 6, 116
- Betts, B. H. 1997, in *Lunar and Planetary Inst. Technical Report*, 28, *Lunar and Planetary Science Conference*, 107
- Blewett, D. T., Lucey, P. G., Hawke, B. R., & Jolliff, B. L. 1997, *J. Geophys. Res.*, 102, 16319
- Conel, J. E. 1969, *J. Geophys. Res.*, 74, 1614
- Gillis, J. J., Jolliff, B. L., & Korotev, R. L. 2004, *Geochim. Cosmochim. Acta*, 68, 3791
- Glotch, T. D., Lucey, P. G., Bandfield, J. L., et al. 2010, *Science*, 329, 1510
- Greenhagen, B. T., Lucey, P. G., Wyatt, M. B., et al. 2010, *Science*, 329, 1507
- Hapke, B. 2001, *J. Geophys. Res.*, 106, 10039
- Howard, K. A. 1973, *Science*, 180, 1052
- Korotev, R. L., Jolliff, B. L., & Rockow, K. M. 1996, *Meteoritics and Planetary Science*, 31, 909
- Korotev, R. L., Jolliff, B. L., Zeigler, R. A., Gillis, J. J., & Haskin, L. A. 2003, *Geochim. Cosmochim. Acta*, 67, 4895
- Kusuma, K. N., Sebastian, N., & Murty, S. V. S. 2012, *Planet. Space Sci.*, 67, 46
- Lawrence, D. J., Feldman, W. C., Elphic, R. C., et al. 2002, *Journal of Geophysical Research (Planets)*, 107, 5130
- Logan, L. M., Hunt, G. R., Salisbury, J. W., et al. 1973, *J. Geophys. Res.*, 78, 4983
- Lucey, P. G., Taylor, G. J., & Malaret, E. 1995, *Science*, 268, 1150
- Lucey, P. G., Blewett, D. T., & Hawke, B. R. 1998, *J. Geophys. Res.*, 103, 3679
- Lucey, P. G., Blewett, D. T., & Jolliff, B. L. 2000, *J. Geophys. Res.*, 105, 20297
- Ohtake, M., Matsunaga, T., Haruyama, J., et al. 2009, *Nature*, 461, 236
- Paige, D. A., Foote, M. C., Greenhagen, B. T., et al. 2010, *Space Sci. Rev.*, 150, 125
- Salisbury, J. W., & Walter, L. S. 1989, *J. Geophys. Res.*, 94, 9192
- Taylor, S. R. 1987, *Geochim. Cosmochim. Acta*, 51, 1297
- Wilcox, B. B., Lucey, P. G., & Gillis, J. J. 2005, *Journal of Geophysical Research (Planets)*, 110, 11001
- Wu, Y. 2012, *Geochim. Cosmochim. Acta*, 93, 214
- Wu, Y., Xue, B., Zhao, B., et al. 2012, *Journal of Geophysical Research (Planets)*, 117, 2001